Simultaneous Absolute Determination of Particle Size and Effective Density of sub-Micron Colloids by Disc Centrifuge Photosedimentometry

Mungai Kamiti[1], David Boldridge[1], Linda M. Ndoping[1], and Edward E. Remsen[2,*]

[1]Cabot Microelectronics Corporation

870 North Commons Drive

Aurora, IL 60504

[2]Mund-Lagowski Department of Chemistry and Biochemistry

Bradley University

1501 West Bradley Avenue

Peoria, IL 61625

ABSTRACT

Disk centrifuge photosedimentometry (DCP) with fluids of different density is used to simultaneously determine the particle size and effective density of spherical silica particles. Incorporation of a calibrated infrared pyrometer into a DCP instrument is shown to enhance the measurement capability of the DCP technique by enabling the correction of the spin fluid's density and viscosity. Key advantages of absolute DCP determinations for size and density analysis relative to standardized DCP measurements include the elimination of instrument standardization with a particle of known density, and measurements or estimation of the effective particle density. The reliability of diameter determinations provided by absolute DCP was confirmed using silica particles with nominal diameters ranging from 250 to 700 nm by comparison of these analyses with diameter determination transmission electron microscopy for silica particle size standards. Effective densities determined by absolute DCP for the silica particles ranged from 2.02 to 2.34 g/cc. These findings indicate that these particles have little or no porosity. The reported characterization of colloidal silica using absolute DCP suggests applicability of the technique to a variety of particle types including colloidal materials other than silica, core-shell particles, compositionally heterogeneous mixtures of nanoparticles, and irregularly shaped, structured colloids.

INTRODUCTION

Increasing use of sub-micron colloids and nanoparticles in emerging materials designed for specific chemical and biochemical applications[1-5] has created a continuing need for new analytical methods of characterization for the particles in these materials. Many particle characterization techniques[6] address this need only partially because these methods typically characterize a single particle heterogeneity, such as the particle size distribution. Since emerging materials often exhibit heterogeneity with respect to size, shape, and chemical composition of their particle components, approaches capable of analyzing multiple heterogeneities of particle distributions are both necessary and important.

Among the well-established particle characterization techniques, centrifugal sedimentation possesses the intrinsic versatility required for the absolute analysis of multiple heterogeneities in particle dispersions. Because the sedimentation rate of a particle in a centrifugal field depends on both the particle size and the density difference between the particle and the sedimentation fluid, centrifugal sedimentation of a particle in two separate sedimentation fluids differing in their density provides a sufficient number of determinations of the particle's sedimentation time for an absolute, simultaneous determination of its size and its effective density.[7] Physical separation techniques based on centrifugal sedimentation, such as sedimentation field-flow fractionation, have also been applied in the simultaneous analysis of particle diameter and effective particle density[8-10].

Sedimentation methods of analysis have been demonstrated as particularly effective in analytical ultracentrifugation studies of macromolecules. Sedimentation equilibrium data collected separately in H_2O and D_2O-based buffers can be combined to provide simultaneous, absolute molecular weight and particle specific volume determination for proteins[11] and organic

nanoparticles[12, 13]. Analogous sedimentation velocity measurements have yielded simultaneous analyses of particle size and effective particle density for polymer lattices[14] and inorganic-organic hybrid colloids[15].

A related technique, disc centrifuge photosedimentometry (DCP),[16] has experienced increasing use in particle size distribution analysis for a wide variety of synthetic and biological materials, including nanotubes,[17] nanocomposites,[18] bacteria,[19] and viruses[20]. The method has been extended recently to incorporate corrections to the measured particle size resulting from particle density variations across the particle size distribution in the case of polystyrene-grafted silica nanoparticles.[21]

An experimental feature common to these successful applications of DCP has been standardization of the disc centrifuge with a particle of known effective density, typically a poly(vinyl chloride) latex. A separate evaluation or estimation of the experimental material's effective density is also required, but standardized DCP measurements collected in spin fluids of different density have also been shown recently to provide an estimate of the effective density of an experimental material.[22] Standardization of the DCP provides significant experimental convenience in that it allows particle size distribution analysis to be performed without accurately knowing the density and viscosity of the spin fluid which is strongly influenced by the frictional heating of the disc under rotation. However, if the spin fluid density and viscosity could be thermally equilibrated and determined accurately through *in-situ* disc temperature measurements prior to a DCP analysis, as is typically done in analytical ultracentrifugation analyses,[11-15] the DCP technique would gain the capability of making simultaneous, absolute determinations of particle size and the effective particle density for sub-micron colloids and nanoparticles.

Modification of a DCP instrument to enable this determination is described. Colloidal silica was chosen as the test material due to its commercial availability in a wide range of sub-micron diameters with narrow particle size distributions. Using H_2O and D_2O-based sucrose gradients as spin fluids in conjunction with temperature equilibration based on accurate and precise *in-situ* measurements of the spin fluid temperature, simultaneous absolute determinations of sub-micron silica particle size distribution and effective particle density were demonstrated. Potential future applications of this technique, including the characterization of other spherical colloidal materials, irregularly-shaped structured particles, and mixtures of interacting nanoparticles are described.

EXPERIMENTAL SECTION

Materials and Sample Preparation. Five colloidal silica ranging in nominal mean particle diameter from 250 nm to 700 nm was purchased from three commercial sources: Duke Scientific Corp., Palo Alto, CA (samples D and E); Bangs Laboratories Inc., Fishers, IN (samples B and C); and Corpuscular Inc., Cold Spring, NY (sample A). A commercial poly(vinyl chloride) latex standard of known diameter (1.403 μm) and effective density (1.385 g/cc) was purchased from CPS Instruments Inc. (Stuart, FL). All samples were used as-received.

De-ionized water (18 MΩ-cm) was filtered through a 0.2 μm filter prior to use. Deuterium oxide (99.96 atom%) and sucrose were purchased from Sigma-Aldrich Inc. (St. Louis, MO). Sucrose was dried overnight under vacuum at 60˚C prior to use. All reagents employed in sample preparation were analytical-grade or better.

Sucrose stock solutions with nominal concentrations of 8 wt% and 24 wt% were prepared in H_2O and D_2O. The actual concentration of sucrose in the solutions was determined experimentally *via* refractometry using a Model AR 700 refractometer (Reichert Analytical Instruments Inc., Depew, NY).

Samples for analysis in D_2O-sucrose gradients were dialyzed exhaustively against pure D_2O using 0.5 mL micro-dialysis cells (Thermo Fisher Scientific Inc., Rockford, IL). Samples were diluted prior to analysis in either de-ionized, filtered H_2O or D_2O to final concentrations ranging from 0.005 wt% to 0.0125 wt%.

Disc Centrifuge Photosedimentation (DCP) Measurements. DCP measurements were performed using a Model DC24000 disc centrifuge (CPS Instruments Inc., Stuart, FL). The disc centrifuge was equipped with a 405 nm diode sensor and was operated at disc speeds between 2,500 to 10,000 rpm. Disc speeds were measured with a Model PT99 tachometer (Monarch Instruments Inc., Amherst, NH, USA) which indicated that disc speeds used in the analysis were

accurate to within ±0.4% of the set value. The radial position of the sensor was determined experimentally by injecting 100 μL aliquots of water into the empty disc spinning at 12,000 rpm. Accumulation of water aliquots in the disc produced a sensor response when the level of injected water reached the position of the sensor allowing the determination of the sensor's radial position from the total volume of injected water into the disc.

Sucrose gradients were generated *in-situ* by filling the empty disc, spinning at the desired speed, with the 8 wt% and 24 wt% sucrose stock solutions which were mixed and pumped into the disc using a Model AG300 automatic gradient builder (CPS Instruments Inc.). The delivered mass of each sucrose stock solution was determined gravimetrically. A 1.0 mL aliquot of *n*-dodecane was injected into the disc to form a thin protective layer on the surface of the sucrose gradient which minimized water evaporation.

Dodecane-capped, sucrose gradients were equilibrated to constant temperature as determined by a Model MI-N500-N infrared pyrometer (Mikron InfraRed Inc., Oakland, NJ) installed inside the disc centrifuge and positioned to measure the heat emitted from the surface of the spinning disc. A detailed description of the installation and operation of the pyrometer can be found in the Supporting Information (page S-2). Standardization of pyrometer prior to use indicated that measured temperatures were accurate to within ±0.5°C of the true temperature. The equilibrium temperature of the spin fluid was taken as the temperature of the disc which reached thermal equilibrium after 45 minutes of spinning at the desired speed before analysis.

Sample aliquots (0.1 mL) were injected into the spinning, thermally equilibrated spin fluid and data acquisition was initiated upon injection. Sample sedimentation time and turbidity at 405 nm were acquired using the instrument's Disc Centrifuge Control System (DCCS)

software. Raw data files were exported for data reduction and analyzed using software written for program **OriginPro 7** (OriginLab Corp., Northampton, MA).

Details of the calculation of sucrose gradient densities and viscosities can be found in the Supporting Information (pages S-3 and S-4).

Calculation of Particle Diameter and Effective Density. Particle diameters, *D*, were calculated from the sedimentation time, t_{sed}, using the well-known dependence of particle diameter on sedimentation time[23]:

$$D^2 = (18/\omega^2 t_{sed})\int[\eta(r)/r\Delta\rho(r)]\mathrm{d}r \quad (1)$$

where: ω is the disc's rotational speed; η is the absolute viscosity of the sedimentation fluid; r is the radius; and $\Delta\rho = \rho_{particle} - \rho_{fluid}$ and is the difference in density between the particle, $\rho_{particle}$, and the sedimentation fluid, ρ_{fluid}.

In disc centrifugation, separation according to particle size and density is achieved by the sedimentation of the particle through a fluid trapped between parallel transparent plates.[23] The quantity of material is determined through optical attenuation of a light source placed near the rim of the disc as a continuous function of sedimentation time.[16, 23]

Because the sedimentation fluid used in this study consisted of three different fluid layers (a sucrose gradient, water (H_2O or D_2O) from injected sample dispersions, and *n*-dodecane), equation 2 included individual contributions from the three fluid layers:

$$\begin{aligned} D^2 = (18/\omega^2 t_{sed})\{&[\eta_{dodecane}\ln(r_o/r_i)/\Delta\rho_{dodecane}] \\ &+ [\eta_{water}\ln(r_o/r_i)/\Delta\rho_{water}] \\ &+ \int[\eta_{sucrose}(r)/r\Delta\rho_{sucrose}(r)]\mathrm{d}r\} \end{aligned} \quad (2)$$

where: r_o and r_i are the outer and inner radii of the specific fluid layer, respectively; $\eta_{dodecane}$ and η_{water}, $\eta_{sucrose}(r)$ are the absolute viscosities of the *n*-dodecane and the water (H_2O or D_2O) and

sucrose layers, respectively; and $\Delta\rho_{dodecane}$, $\Delta\rho_{water}$, $\Delta\rho_{sucrose}(r)$ are the differences in density between the particle and the respective fluid layers. The integral in equation 2 corresponds to the sucrose gradient and it was evaluated numerically after substitution of the appropriate polynomial expressions for the dependence of gradient's viscosity and density on the radius.

Measured turbidity at 405 nm was converted to the number of particles (n_i) for each measured diameter (D_i) by treating the particles as spherical Mie scatterers with no optical absorbance at the incident wavelength.[24] A value of 1.45 at 405 nm was taken as an estimate of the refractive index for colloidal silica[25] and used in the calculation of n_i. The refractive index of the H_2O-sucrose gradient at the radius corresponding to the sensor position was estimated from the determined sucrose concentration at the sensor position and literature values for the refractive index of H_2O-sucrose solutions[26]. The corresponding refractive index of the D_2O-sucrose solutions at the sensor position were estimated from refractive index of H_2O-sucrose solutions corrected for the refractive index difference between H_2O and D_2O[27].

The calculated number-mean particle diameter, D_n of a particle size distribution was given by:

$$D_n = \sum n_i D_i / \sum n_i \quad (3)$$

The corresponding weight-mean diameter, D_w, was given by[28]:

$$D_w = \sum n_i D_i^4 / \sum n_i D_i^3 \quad (4)$$

The effective density was determined by iteratively calculating the particle size distribution from the sedimentation data. The particle density which resulted in the same calculated particle size distribution for both spin fluids was taken as the effective density. Reported values of D_w, D_n, and effective density for individual silica samples are the mean

values obtained by averaging D_w, D_n, and effective density results obtained from triplicate determinations collected at a minimum of two disc speeds per sample.

The same experimental data sets used to determine particle diameter via the absolute DCP method were also used to evaluate mean particle diameters using the standardized DCP method[16].

RESULTS AND DISCUSSION

Analysis of Particle Size and Effective Density. Disc centrifuge photosedimentometry data collected in H_2O-sucrose and D_2O-sucrose gradients are shown in Figure 1 for a size-certified colloidal silica standard (sample D). Particle sedimentation was shifted to longer times in the D_2O-sucrose gradient compared to sedimentation in the H_2O-sucrose gradient due to the increased density and viscosity of D_2O relative to H_2O.

Representative results for particle diameters calculated as a function of effective particle density for runs collected in H_2O-sucrose and D_2O-sucrose gradients are shown for samples C and D in Figure 2. Quadratic fits to the data sets exhibited a crossing point for each pair of analyses which corresponded to the simultaneously determined value of the respective particle's weight-mean diameter and its effective density.

Particle size distributions for the set of silica samples exhibited varying degrees of broadening and/or bimodality as shown in Figure 3 for samples A and D. The minor modes of sample A and sample D centered at 291 and 568 nm, respectively, correspond to Stokes dimers of their primary particle peak diameters of 243 and 473 nm, respectively. Mean particle diameters and effective densities and their associated uncertainties for all samples are summarized in Table 1. Particle diameter determinations by standardized DCP are also summarized in Table 1.

The accuracy of the absolute DCP method was assessed from a determination the absolute error based on the comparison of mean number-mean diameters determined for samples D and E, which were size-certified particle standards, with the corresponding transmission electron microscopy (TEM) diameters stated on the particle supplier's certificate of analysis. The specified TEM diameter for sample D was 490 $\pm$ 30 nm and the corresponding diameter for

sample E was 730 ± 40 nm. Comparison of the TEM diameters with mean number-average diameters determined by absolute DCP yielded an absolute error of 4.1% and 2.6% for samples D and E, respectively, resulting in an average absolute error of 3.4% for the DCP method.

The reliability of densities determined by absolute DCP was evaluated by comparing mean weight-average diameters (D_w) determined by absolute DCP with the values of D_w obtained by standardized DCP, as summarized in Table 1. The values of D_w for standardized DCP were calculated using the effective particles densities reported in Table 1. A mean absolute difference of 2.5% was found between the respective values of D_w which was within the experimental uncertainty of the two DCP methods. Because the determination of standardized DCP diameters relies on calibration of particle sedimentation time with a poly(vinyl chloride) latex particle of significantly different effective density (1.385 g/cc) than silica, the 2.5% mean difference between the values of D_w indicates reliability for the analysis of effective particle densities by absolute DCP. This interpretation was tested further through a re-calculation of standardized DCP using a constant particle density of 2.0 g/cc for the sample set. As expected, the particle diameters increased. For example, the weight-average diameter obtained via standardized DCP with a constant particle density of 2.0 g/cc for sample A (280 nm) exceeded the corresponding value obtained by absolute DCP (247 nm) by 13.4%. This finding highlights the importance of using reliable effective densities in the determination of accurate particle diameters *via* the standardized DCP method.

Comparison of absolute DCP data for the set of samples in Table 1 revealed a trend between measured diameters and effective particle densities in which the effective particle densities increased with decreasing particle diameter. This trend is depicted graphically in Figure 4. The five silica samples formed two groups, one with the larger diameter particles, sample D

and sample E, having a lower mean effective density of 2.06 $\pm$ 0.06 g/cc, and a second group with smaller diameter particles, samples A, B, and C, having a higher mean effective density of 2.27 $\pm$ 0.09 g/cc. Particle densities for colloidal silica are known to be process-specific, as in the case of Stöber silica for which the particle density ranges from 1.87 to 2.1 g/cc.[29] Increasing density for smaller silica particles relative to larger silica particles is consistent with previous standardized DCP characterizations of Stöber silica particles in which particles smaller than 260 nm in mean diameter exhibited higher effective particle density than particles that were larger in mean diameter.[22]

The effective densities of colloidal silica particles determined in the present study fell within $\pm$ 0.2 g/cc of the nominal density of solid amorphous silica which is 2.2 g/cc.[30] The magnitudes of the effective densities determined in the present study relative to the nominal density of solid amorphous silica suggest that the samples were minimally porous or non-porous.

Potential Applications to Other Particles. **S**pherical colloids and nanoparticles prepared from materials other than silica are amenable to analysis by the absolute DCP method provided the particle's effective density falls within the range appropriate for the H_2O-sucrose, D_2O-sucrose gradient combination. The particle's effective density must be greater than *ca.* 1.2 g/cc which corresponds to the approximate room temperature density of the D_2O-sucrose gradient at the maximum sucrose concentration (24 wt%). Application of the method to particles of high effective density requires that density difference between the two gradients produces a measurable difference in sedimentation times for the particle. The colloidal silica used in this study exhibit a range of effective densities approaching the upper limit for which the H_2O-sucrose, D_2O-sucrose gradient combination is effective.[14, 22, 31] Representative particle types meeting the requirements with respect to the particle's effective density relative to the sucrose

density gradients include particles with broad or multi-modal size distributions, composite core-shell nanomaterials[21] and irregularly-shaped structured particles[32]. The absolute DCP technique could also be applied productively in further analyses of the correlation between particle size and particle diameter of silica colloids. This approach may better elucidate the dependence of particle porosity on the synthetic methods used in silica colloid synthesis. Finally, additional development of the technique for the determination of heterogeneity in particle density as a function of particle diameter may enable the analysis of interactions in between nanoparticles or colloids of differing chemical composition.

CONCLUSIONS

Simultaneous absolute determination of particle size and effective particle density of colloids using disc centrifuge photodensitometry is demonstrated. This enhanced capability is attributable to the installation of a calibrated infrared pyrometer inside the DCP instrument which enables careful thermal equilibration of the spin fluid in the rotating disc. The temperature measurements additionally allowed accurate determinations of the density and viscosity of the spin fluid for DCP data collected separately in H_2O-sucrose and D_2O-sucrose gradients. The measured effective densities of colloidal silica test particles approached the density of solid amorphous silica, suggesting that these particles have little if any porosity. The feasibility of absolute DCP measurements for particle size and effective density of silica colloids points to a broad applicability of the method for colloidal materials other than silica, irregularly-shaped structured particles, and mixtures of compositionally heterogeneous, interacting nanoparticles.

ACKNOWLEDGEMENTS

The authors thank T. Werts for the installation of the infrared pyrometer and for measurements of the disc speed. Permission given by Cabot Microelectronics Corporation to publish this work is gratefully acknowledged

REFERENCES

1. Husein, M. M.; Nassar, N. N. *Curr. Nanosci.* **2008,** *4*, 370-380.
2. Sharma, V. K.; Yngard, R. A.; Lin, Y. *Adv. Colloid Interface Sci.* **2009,** *145*, 83-96.
3. Subbiah, R.; Veerapandian, M.; Yun, K. S. *Curr. Med. Chem.* **2010**, 17, 4559-4577
4. Liu, Y.; Welch, M. J., *Bioconj. Chem.* **2012**, 23, 671-682.
5. Tourbin, M.; Frances, C. *Part. & Part. Syst. Charact.* **2007,** *24*, 411-423.
6. Kirkland, J. J. *Surfact. Sci. Ser.*, **2006,** *131*, 537-548.
7. Daily, J. W.; Harleman, D. R. F. In *Fluid Dynamics*, Addison-Wesley Publishing Co. Inc.: 1965.
8. Giddings, J. C.; Moon, M. H.; Williams, P. S.; Myers, M. N. *Anal. Chem.* **1991,** *63*, 1366-1372.
9. Giddings, J. C.; Moon, M. H. *Anal. Chem.* **1991,** *63*, 2869-2877.
10. Giddings, J.; Ratanathanawongs, S. K.; Barman, B. N.; Moon, M. H.; Guangyue, T.; Hansen, M. E. *Adv. Chem. Ser.* **1994,** *234*, 309-340.
11. Edelstein, S. J.; Schachman, H. K. *J. Biol. Chem.* **1967,** *242*, 306-311.
12. Remsen, E. E.; Thurmond, K. B.; Wooley, K. L. *Macromolecules* **1999,** *32*, 3685-3689.
13. Tziatzios, C.; Precup, A. A.; C. H. Weidl, C. H.; Schubert, U. S.; Schuck, P.; Durchschlag, H.; Mächtle, W.; van den Broek, J. A.; Schubert, D. *Prog. Colloid Polym. Sci.* **2002,** *119*, 24-30.
14. Müller, H. G.; Hermann, F. *Prog. Colloid Polym. Sci.* **1995,** *99*, 114-119.
15. Cölfen, H. Völkel, A. *Prog. Colloid Polym. Sci.* **2006,** *131*, 126-128.
16. Fitzpatrick, S. T. *Polym. News* **1999,** *24*, 42-50.

17. Nadler, M.; Mahrholz, T.; Riedel, U.; Schilde, C.; Kwade, A. *Carbon* **2008,** *46*, 1384-1392.

18. Fielding, L. A.; Tonnar, J.; Armes, S. P. *Langmuir* **2011**, *27*, 11129-11144.

19. Thomas, J. C.; Middelberg, A. P. J.; Hamel, J-F.; Snoswell, M. A. *Biotechnol. Prog.* **1991,** *7*, 377-379.

20. Bondac, L. L.; Fitzpatrick, S. *J. Ind. Microbiol. Biotechnol.* **1998,** *20*, 317-322.

21. Fielding, Lee A.; Mykhaylyk, O. O.; Armes, S. P.; Fowler, P. W.; Mittal, V.; Fitzpatrick, S. *Langmuir* **2012**, *28*, 2536-2544.

22. Bell, N. C.; Minelli, C.; Tompkins, J.; Stevens, M. M.; Shard, A. G. *Langmuir* **2012,** *28*, 10860-10812.

23. Daily, J. W.; Harleman, D. R. F. In *Fluid Dynamics*, Addison-Wesley Publishing Co. Inc.: 1965.

24. van de Hulst, H. C. *Light Scattering by Small Particles*, p. 135, Dover Publication Inc.: New York, 1981.

25. Iler, R. K. *The Chemistry of Silica: Solubility, Polymerization, Colloid and Surface Properties, and Biochemistry*, Wiley: New York, 1979.

26. Weast, R. C. (ed.) *CRC Handbook of Chemistry and Physics*, 64th ed.; CRC Press: Boca Raton, 1983.

27. Odhner, H.; Jacobs, D. T. *J. Chem. Eng. Data* **2012,** *57*, 166-168.

28. R. R. Irani, R. R.; Callis, C/ F. *Particle Size: Measurement, Interpretation and Application*, pp. 43-45, Wiley: New York, 1963.

29. Domingos, R. F.; Baaloousha, M. A.; Ju-Nam, Y.; Reid, M. M.; Tufenkji, N.; Lead, J. R.; Leppard, G. G.; Wilkinson, K. J. *Environ. Sci. Technol.* **2009,** *43*, 344-361.

30. Iler, R. K. *The Chemistry of Silica: Solubility, Polymerization, Colloid and Surface Properties, and Biochemistry,* Wiley: New York, 1979.

31. Planken, K. L.; Colfen, H. *Nanoscale* **2012,** *2,* 1846-1869.

32. Gregory, J. *Wat. Sci. Tech.* **1997,** *36,* 1-13.

SUPPORTING INFORMATION AVAILABLE

Additional information is referenced in the text. This material is available free of charge via the internet at http://pubs.acs.org.

Table 1

Effective Density and Mean Particle Size Distribution Averages for Colloidal Silica Samples

Sample	D_n[a] (nm)	D_w[a] (nm)	Density (g/cc)	D_n[b] (nm)	D_w[b] (nm)
A	246 ± 7	247 ± 7	2.34 ± 0.07	237 ± 2	239 ± 3
B	249 ± 4	251 ± 4	2.25 ± 0.03	243 ± 2	244 ± 2
C	408 ± 7	412 ± 8	2.23 ± 0.04	395 ± 7	403 ± 6
D	470 ± 10	476 ± 11	2.10 ± 0.06	462 ± 3	468 ± 5
E	748 ± 10	754 ± 10	2.02 ± 0.02	719 ± 12	734 ± 6

[a] Diameter determined by simultaneous analysis in H_2O and D_2O sucrose gradients.

[b] Diameter determined by standardized DCP analysis using effective density determined in H_2O and D_2O sucrose gradients.

FIGURE CAPTIONS

Figure 1. Normalized centrifugal sedimentation data for sample A in H_2O-sucrose gradient (solid line) and in D_2O-sucrose gradient (dashed line). Turbidity at 405 nm was normalized to the peak turbidity of the respective data set. Disc speed for both data sets was 10,000 rpm.

Figure 2. Dependence of the weight-mean particle diameter (D_w) on the effective particle density for sample C (circles) and sample D (squares) analyzed in H_2O-sucrose (solid symbol) and D_2O-sucrose (open symbol) gradients. Quadratic fits to the H_2O data are represented by the solid lines. Quadratic fits to the D_2O data are represented by the dashed lines. The crossing points of the fitted curves are indicated by the two arrows. Disc speed for the sample C and the sample D data sets was 10,000 and 7,500 rpm, respectively.

Figure 3. Overlay of number-mean particle size distributions for sample A (solid line) and sample B (dashed line) analyzed in a D_2O-sucrose gradient and calculated with measured effective particle densities of 2.34 and 2.10 g/cc, respectively. Disc speed used for both analyses was 7,500 rpm.

Figure 4. Dependence of the measured effective particle density on the weight-mean diameter, D_w. Error bars shown are $\pm$ 1σ limits about the mean values represented by the solid circles.

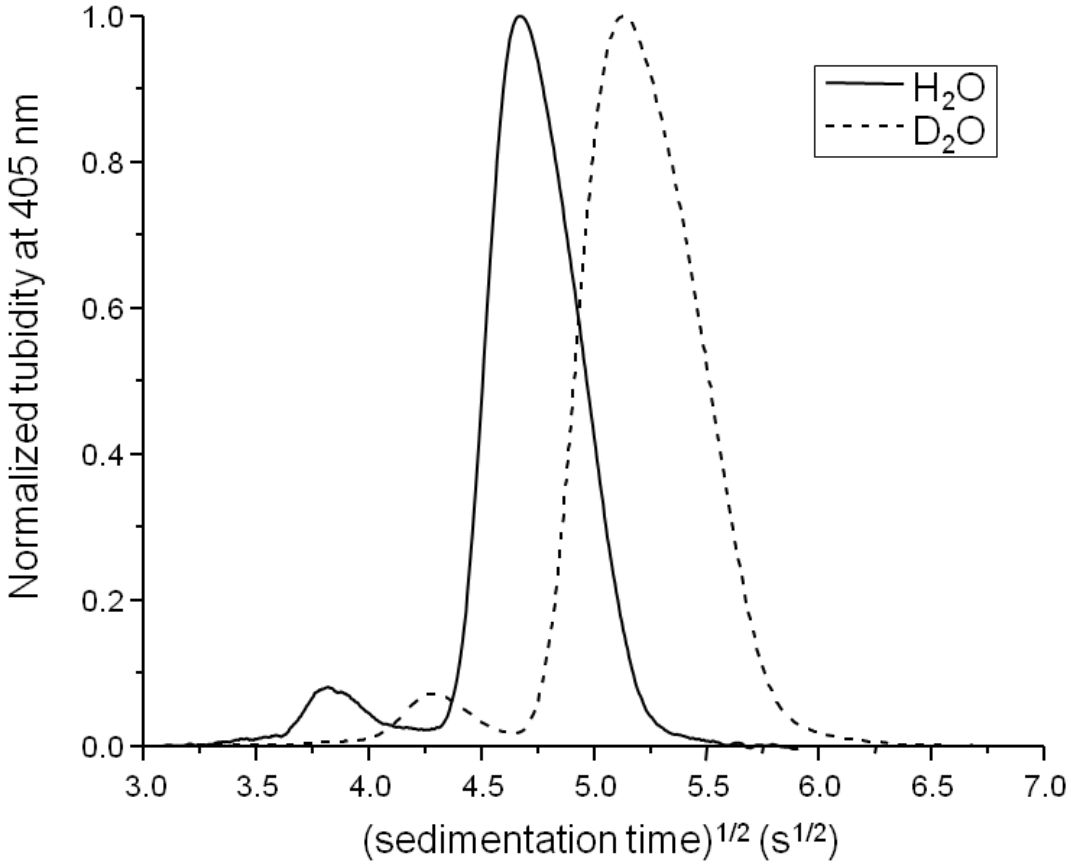

Figure 1. Normalized centrifugal sedimentation data for sample A in H_2O-sucrose gradient (solid line) and in D_2O-sucrose gradient (dashed line). Turbidity at 405 nm was normalized to the peak turbidity of the respective data set. Disc speed for both data sets was 10,000 rpm.

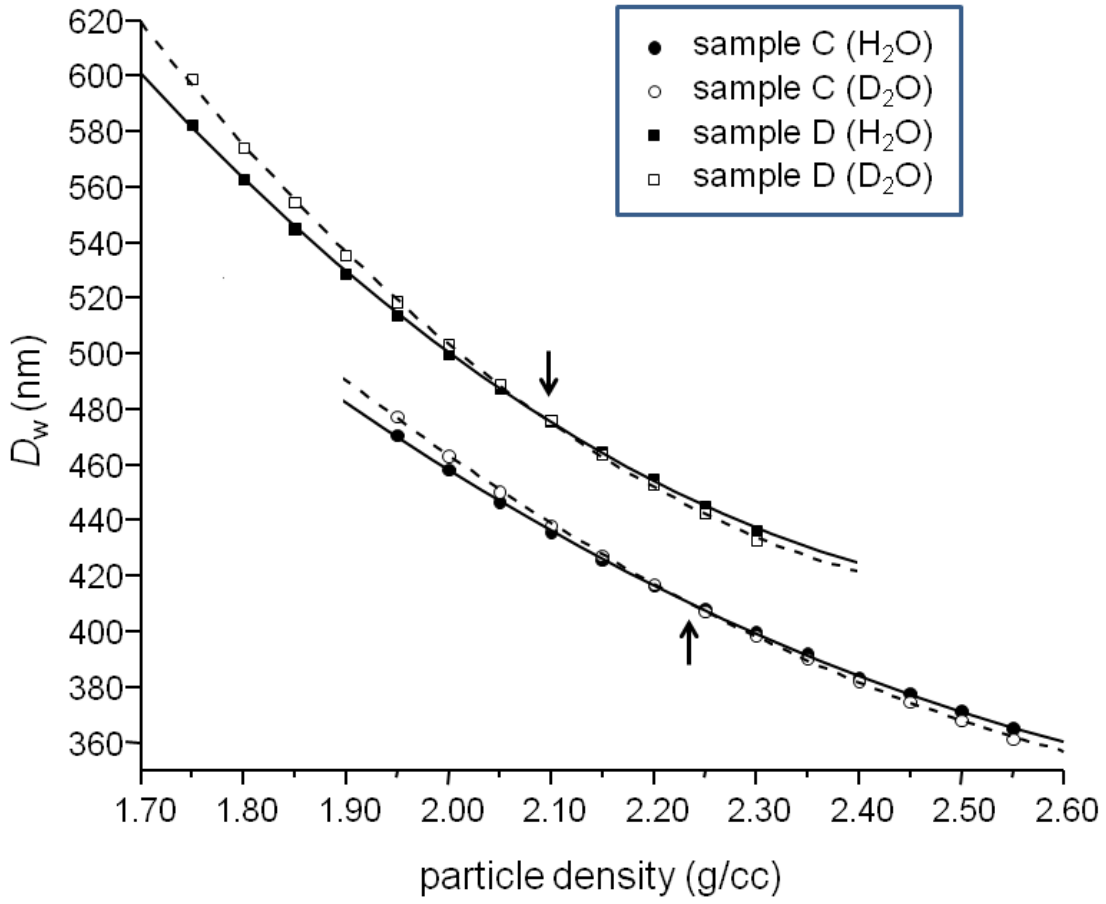

Figure 2. Dependence of the weight-mean particle diameter (D_w) on the effective particle density for sample C (circles) and sample D (squares) analyzed in H_2O-sucrose (solid symbol) and D_2O-sucrose (open symbol) gradients. Quadratic fits to the H_2O data are represented by the solid lines. Quadratic fits to the D_2O data are represented by the dashed lines. The crossing points of the fitted curves are indicated by the two arrows. Disc speed for the sample C and the sample D data sets was 10,000 and 7,500 rpm, respectively.

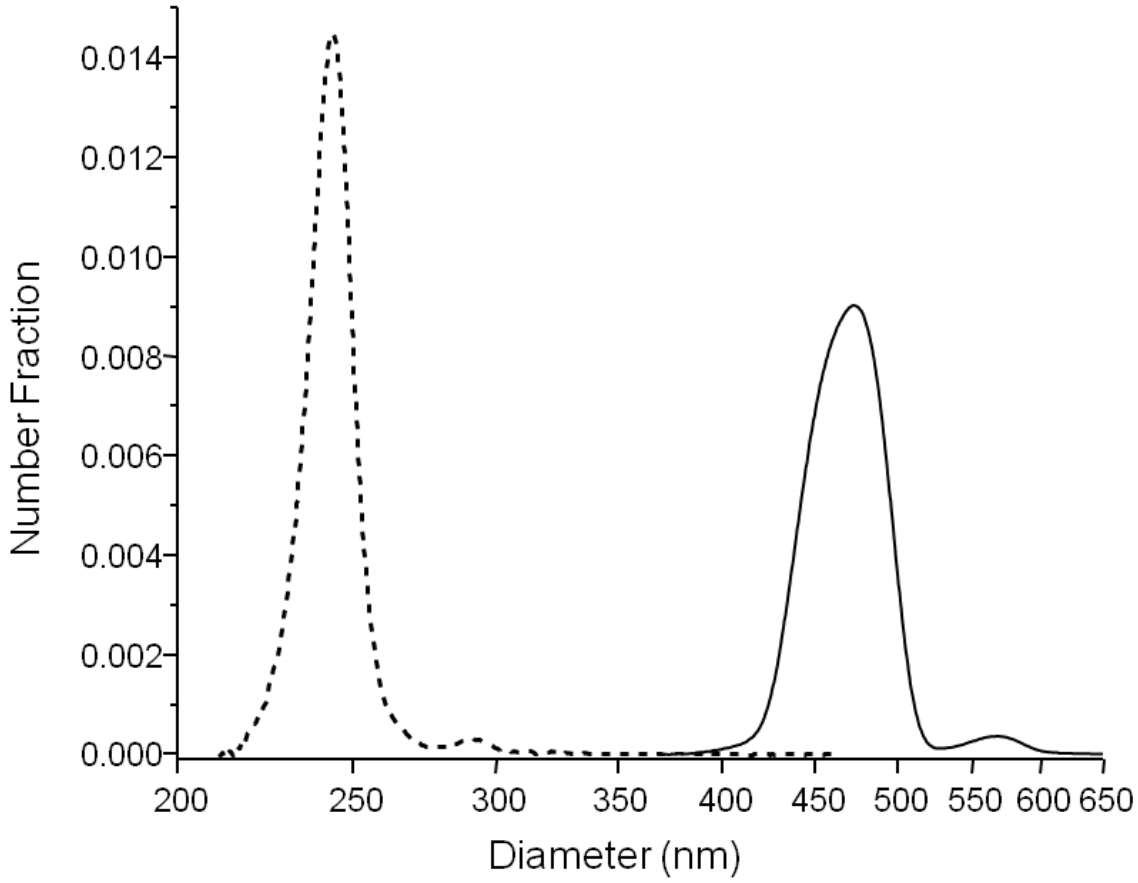

Figure 3. Overlay of number-mean particle size distributions for sample A (solid line) and sample B (dashed line) analyzed in a D_2O-sucrose gradient and calculated with measured effective particle densities of 2.34 and 2.10 g/cc, respectively. Disc speed used for both analyses was 7,500 rpm.

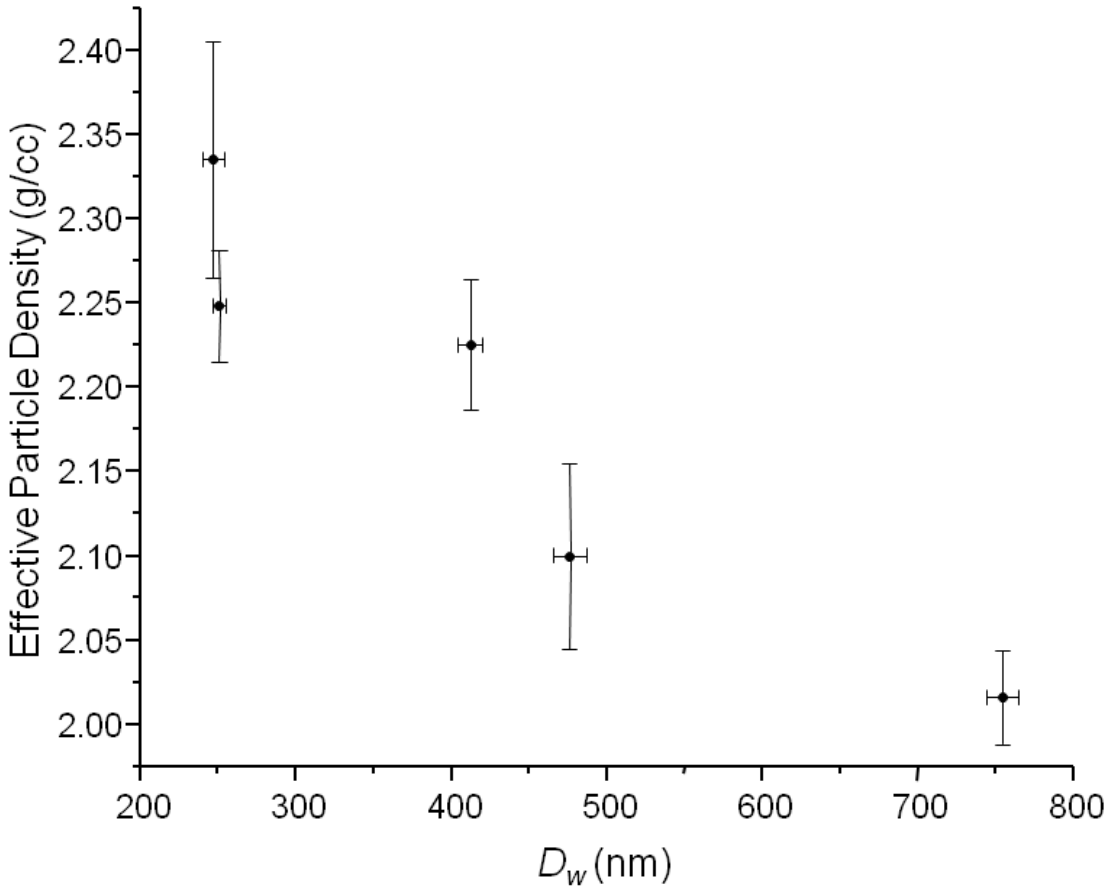

Figure 4. Dependence of the measured effective particle density on the weight-mean diameter, D_w. Error bars shown are $\pm$ 1σ limits about the mean values represented by the solid circles.